Research Square

Preprints are preliminary reports that have not undergone peer review.
They should not be considered conclusive, used to inform clinical practice,
or referenced by the media as validated information.

Hsa-MiR-590-3p promotes the malignancy progression of pancreatic ductal carcinoma cell by inhibiting the expression of p27 and PPP2R2A via G1/S cell cycle pathway

Xiaoyang Shi
China Medical University First Hospital
Weiwei Sheng
China Medical University First Hospital
Chao Jia
China Medical University First Hospital
Jingtong Tang
China Medical University First Hospital
Ming Dong (dongming@cmu.edu.cn)
China Medical University First Hospital https://orcid.org/0000-0003-2685-1420

Primary research

Keywords: MiR-590-3p, pancreatic ductal carcinoma, p27, PPP2R2A, G1/S cell cycle pathway

Posted Date: May 12th, 2020

DOI: https://doi.org/10.21203/rs.3.rs-27360/v1

License: This work is licensed under a Creative Commons Attribution 4.0 International License.
Read Full License

Abstract

Background: miR-590-3p plays an important role in the occurrence and development of many cancers, but its role in pancreatic cancer has not been reported.

Objective: Investigate the effect and target genes of miR-590-3p in pancreatic cancer, so as to provide new diagnostic and therapeutic ideas for pancreatic cancer.

Methods: qRT-PCR, MTT, clonal formation assay, flow cytometry and transwell assay were used to detect malignant cell behaviors. TargetScan (http://www.targetscan.org) was used to predict the binding region of miR-590-3p to target genes. Immunohistochemistry and Western blot were used to detect protein expression.

Results: hsa-miR-590-3p expressed significantly higher in PC tissues than paired normal pancreas and its expression level was associated with PC tumor size (P=0.042) and preoperative CA19-9 level (P=0.046). Its overexpression promoted PC cell proliferation, invasion and migration following with the p27 and PPP2R2A protein down-regulation, and vice versa. Dual-luciferase reporter assay confirmed that p27 and PPP2R2A were direct target genes of miR-590-3p. Overexpression of P27 and PPP2R2A reversed the promoting effect of miR-590-3p on cell proliferation, migration and invasion.

Conclusion: MiR-590-3p promote the development of pancreatic cancer by directly downregulated p27 and PPP2R2A via the G1/S cell cycle pathway.

Background

It is a common sense that pancreatic carcinoma (PC) is a member of the most aggressive malignant tumors and contributes to cancer related death as the seventh common cause [1]. It is crucial to identify a new potential biomarker as a prognostic factor and therapeutic target of PC.

MiRNAs as a group of short (~22 nucleotides), endogenous and non-coding RNAs can regulate target gene expression by directly binding to the 3'UTR of specific mRNA[2]. miRNAs are becoming important biomarkers in different kinds of diseases, not only in malignant tumor cells but also in cardiosphere-derived stem cells [3], human mesenchymal stem cell[4] etc. Several microRNAs have been reported to contribute to the tumorigenesis, development and prognosis of PC which might provide therapeutic target for this mortal disease [5].

Has-miR-590-3p is one of the mature members of the human microRNA-590 family. It has been reported that miR-590-3p is related to the development of several kinds of cancer, including colorectal cancer (CRC) [6], Lynch syndrome (a common hereditary form of CRC) [7], glioblastoma[8] and nephroblastoma[9]. However, the effect of miR-590-3p in PC cells has not been reported to our knowledge. In current study, we first discovered that miR-590-3p directly regulated p27 and PPP2R2A in PC cells.

P27 (CDKN1B) belongs to the CIP/KIP family of CDK inhibitors (CDKIs) with p21 and p57, can induce the G1 cell phase arrest by inhibiting cyclin/CDK complexes in a number of cell lines[10]. Posttranscriptional loss of p27 related to poor prognosis in several solid tumors. Reduced expression or loss of p27 protein contributes to the genesis or progression of PC[11-13].

Proteinphosphatase 2A (PP2A) is an important member of the major Ser/Thr phosphatases and belongs to the PPP family involving control of cell growth and division[14; 15].PPP2R2A, also known as PR55αor B55α, has a widespread tissue distribution[14].It has been reported to be a tumor suppressor in seceral kinds of malignant tumors, such as AML, HCC, colorectal cancer, pancreatic cancer.

In our study, the potential function and corresponding molecular mechanism of miR-590-3p in development of PC has been investigated detailedly.

Materials And Method

Human Tissue Specimens

60 paired fresh PC and normal pancreas tissues were obtained from PC patients in the Department of Gastrointestinal and Hernia Surgery of the First Hospital of China Medical University from 2006 to 2017 and 42 pairs fresh tissues of them were stored under -80℃ condition until used. Pathological diagnosis of PC is the necessary condition for all patients to be chosen. This study was approved by the institutional review board of the China Medical University and a consent form was signed by each participating patient. The staging standard was referred to the AJCC Cancer Staging Manual (8th Edition).

Immunohistochemistry（IHC）

All surgical samples were fixed in neutral formaldehyde and embedded in paraffin to make slices 4 um thick. S-P immunohistochemistry was used dyeing. Primary antibody was incubated overnight at 4℃ with rabbit polyclonal p27;KIP antibody (Cat.No.25614-1-AP, 1:200, Proteintech, China) and Rabbit Anti-PPP2R2A antibody(ab18136, 1:100, Abcam, Britain) .Biotin-labeled secondary antibodies (Ultrasensitive; Incubation at indoor temperature for 25min, MaiXin, gentle, China) and display the colors in DAB. 5 fields were randomly selected for each slice. The expression of p27 and PPP2R2A was divided into 5 grades according to the percentage of dyeing area: 0 points (no staining), 1 points (1%~25%), 2 points (26%~50%), 3 points (51%~75%), and 4 points (76% +).The expression of p27 and PPP2R2A was further divided into four grades according to the intensity of staining: 0 (no staining), 1 (pale yellow granules), 2 (dark yellow granules) and 3(yellow-brown granules). The product of the extent and intensity score was used as the final staining scores (0–12).

Cell lines and culture

Human pancreatic cancer（PC）cells BxPC-3, AsPC-1, SW1990 and PANC-1 were purchased from the Cell Bank of the Chinese Academy of Sciences (Shanghai, China). Capan-2 and Miapaca-2 cells were purchased from the American Type Culture Collection (ATCC, USA). And the HEK-293 cell was kindly provided by the Cell Biology Department of China Medical University. All cells were cultured in DMEM or RPMI-1640 within 10 % FBS (Hyclone, Logan, UT, USA), and 1% penicillin streptomycin combination under the condition of 5% CO2 at 37℃ in incubator.

Total RNA isolation and qRT-PCR

We use TRIZOL reagent (Takara Bio, Otsu, Japan) to extract total RNA from tissue samples and harvested PC cells, following the instruction of manufacturer. RNA levels was kept to be equal quantities in all samples via nucleotide test before qRT-PCR detection. MirVana miRNA Isolation Kit (Ambion, Austin, TX) was used to purify microRNAs. For reverse transcriptasepolymerase chain reactions (RT-PCR), we used the stem-loop primer and the PrimeScript RT Reagent Kit (Promega, Madison, WI) to synthesize cDNA. MiRNA primers for qPCR were purchased from GenePharma(Soochow, China). We used the Custom gene qRT-PCR Quantitation Kit (GenePharma) to measure mature miR-590-3p expression under the following thermos cycling conditions: 95℃ for 3 minutes, 45 cycles of 95℃ for 12s and 62℃ for 50 s; and dissociation-curve analysis was added at the end. The relative miR-590-3p expression levels were standardized to U6 snRNA expression, and we use the $2^{-\Delta\Delta ct}$ method to calculate the fold-changes in expression. We defined positive value of ΔΔct as relative miR-590-3p high-expression and negative value of ΔΔct as relative miR-590-3p low-expression (PC tissues comparing with paired normal pancreas tissues).

Primers were as followings:

miR-590-3p forward, 5’-AAAGATTCCAAGAAGCTAAGGGTG-3’and reverse, 5’-CCTAACTGGTTTCCTGTGCCTA-3’; U6 forward,5’-CTCGCTTCGGCAGCACA-3’ and reverse, 5’-AACGCTTCACGAATTTGCGT)-3’.

MiRNA transfection

MiR-590-3p mimics, NC, inhibitors and inhibitor N.C were produced by GenePharma(Soochow, China). For transient expression studies, PC cells were infected with miR-590-3p mimics, NC, inhibitors and inhibitor N.C according to the recommended protocol. Lipofectamine 3000 reagent (Invitrogen, Carlsbad, CA) was the transfection medium during the transfection process.

Cell Cycle

PC cells on culture plate were washed by PBS for twice and collected into centrifuge tubes. 1 ml 70% precooled ethanol were added into centrifuge tubes and kept in tubes at 4°C for 12h. Then, the cells were centrifuged at the condition of 1000rps for 5mins and washed with PBS and centrifuged again under the same condition. The centrifugal sediment was treated with Cell Cycle and Apoptosis Analysis Kit

(Beyotime, China). Flow cytometry was performed to detect the cells 30mins after PI staining. We used cell cycle matching software to analyze the primary result to record hypodiploid peak, namely sub-G1 phase, G0/G1 phase, S phase, and G2/M phase. The experiment was repeated three times independently.

Colony formation and Proliferation assay

1×10^3cells were seeded into 6-well culture plates per well. After 10 days' culturing under the condition of 37 ℃ and 5% CO2 in incubator, the plates were washed with PBS. We washed the cells with PBS twice after fixing them with precooled methanol for 30min and staining them with 1% crystal violet for 30min. We use MTT assay to detect cell proliferation. Briefly, we harvested cells with 0.05 % trypsin/EDTA and counted them after transfection (miR-590-3p mimics, NC, inhibitors and inhibitor NC) for 48h and then seeded them into four 96-well plates at a density of 3,000 cells per well and incubated for overnight. The cells were added within 15μl MTT solution (5 mg/ml in PBS; Sigma) and incubated for 4 h at 37 °C. Then we removed the liquid and added 150μl dimethyl sulphoxide (Sigma) into each well. The absorbancy value(with OD490nm) was detected every 24h for 4 days by ELISA 96-well microtiter plate reader (BIORAD680; USA) and data are presented as the cell number. Three independent experiments were performed.

Cell Migration and Invasion Assay

In our lab, Modified Boyden chamber (BD Biosciences, Sparks, MD, USA) assays are standard assays to assess cell invasion and cell migration. Briefly, miR-590-3p mimics, NC, inhibitors and inhibitor N.C were transfected into PC cells for 48 h. Then 5×10^4cells in 300μl FBS-free culture medium were counted and seeded on BD chamber membrane (pore size: 8.0-μM) in 24-well plates within 600μl culture medium plus 10%FBS in the bottom of each well. Then, 24h later, we used cotton swab to carefully clean cells inside of the chamber. Cells out of the chamber on the bottom were fixed with precooled methanol for 30min, stained with 1% crystal violet for 30min, and washed with PBS twice. We used a microscope (Nikon Microphot-FX, Japan) to take pictures of the migratory cells and count them in five random fields at ×20 magnification. The invasion assay was almost the same with migration assay except that we added 50ul 10% matrigel (BD Biosciences) diluted with FBS-free medium inside the BD chamber on the membrane and incubate the chambers for 4h at 37℃. We counted the actual number of cells per field to present results. Three independent experiments were performed.

Western blot assays

RIPA buffer (Beyotime, China) with 1%PMSF was used to extract total protein. Total proteins (30mg/lane) were divided into peptide chains of different molecular weights by 10% SDS-PAGE electrophoresis (KeyGEN BioTECH, China) and transferred to PVDF membranes (Millipore, Billerica, MA). All the membranes were blocked with 5% nonfat milk for 2h and then incubated with primary antibodies at 4°C overnight, and then the membranes were incubated by a secondary antibody for 2h. BeyoECL Plus reagent (Beyotime, China) was used to detect signals.

Dual-Luciferase Reporter Assay

The p27 and PPP2R2A 3'-UTR sequence were cloned into the pmirGLO vector dividedly. We cotransfected 100ng wild-type or mutant-type firefly luciferase reporter plasmid and 10ng pRL-TK plasmid as control and miR-590-3p mimics or NC into 293 cells reached 50%-80% confluence grown in 12-well plates. Dual-Luciferase Reporter Assay System (Promega) was used to detect luminescence of cells' lysate after culturing cells for 48h. Independent experiments were repeated for 3times.

Statistical Analysis

Statistical analysis was performed with the SPSS software (version 17.0, SPSS Inc., Chicago, IL, USA). Means ± SD was calculated and two tailed Student's t-test was performed using the data analysis tools provided by the software. $P<0.05$ was considered as statistically significant.

Results

MiR-590-3p relatively high-expressed in clinical tumor samples

Hsa-miR-590-3p expression quantities in 42 paired PC and normal pancreas tissues were measured by qRT-PCR. The findings indicated miR-590-3p expression quantities relatively expressed higher in PC tissues than paired normal pancreas(P□0.05, Figure 1a). High expression of miR-590-3p was significantly relevant with tumor size (P=0.042) and high expression of preoperative CA19-9 level(P=0.046), but not related to age, tumor location, gender, the degree of tumor differentiation, UICC stage, lymph node metastasis or postoperative liver metastasis(Table 1). These results above showed that miR-590-3p up-regulation might influence tumor growth of PC cells.

MiR-590-3p enhanced proliferation of PC cells in vitro

We had chosen high miR-590-3p expression (Capan-2) cells and low miR-590-3p expression (PANC-1) cells to continue our following experiments after we measure our 6 PC cells' miR-590-3p expression levels. (Figure 1b).MiR-590-3p mimics and inhibitors were used to investigate the function of this microRNA. The overexpression and silencing efficiency of miR-590-3p in PC cells were confirmed by qRT-PCR (Figure 2a-b). MiR-590-3p overexpression significantly enhanced both two PC cell lines' proliferation and vice versa (Figure 2c -f). Flow cytometry was used to examine the DNA profiles in the two cell lines. The cell cycle distribution of miR-590-3p overexpression group significantly differed from the control group with less G1 phase and higher S+G2 phase (Figure 2g), whereas the inhibition group had an opposite result compared with NC group (Figure 2h). These findings showed that miR-590-3p promoted PC cells proliferation by changing cell cycle proportions.

MiR-590-3p enhanced migration and invasion abilities of PC cells.

Transwell assays indicated that overexpression of miR-590-3p promoted the PC cell migration and invasion compared with NC group (Figure 3a-b), and vice versa (Figure 3c-d).

MiR-590-3p can directly target p27 and PPP2R2A in PC cells and was negatively related to p27 and PPP2R2A in clinical tumor samples

So as to reveal the corresponding mechanism of hsa-miR-590-3p function in PC cells, we use the bioinformatics tool TargetScan (http://www.targetscan.org) to identify the possible target genes of miR-590-3p. Finally, we find p27 and PPP2R2A mRNA as possible direct targets of miR-590-3p. WB showed that miR-590-3p overexpression upregulated p27, PPP2R2A, p21 and ZO-1 expression in Capan-2 cells, but downregulated cyclin E2 and CDK2 expression (Figure 4a). The opposite results were found in cells transfected with inhibitors (Figure 4b). It is the same in PANC-1 cells (Figure 4c-d) .We predicted potential binding sequences on 3' untranslated regions (UTR) of p27 and PPP2R2A with miR-590-3p via TargetScan (Figure 4e) and used dual-luciferase reporter assay to detect relative luciferase intensity of HEK-293 cells cotransfected with miR-590-3p or NC and luciferase reporter plasmid of two target genes. Relative luciferase activity was declined 57.28% and 42.11% within wild type 3 'UTR transcripts of p27 and PPP2R2A, respective compared to negative control group ($p<0.0001$). However, relative luciferase activity was rebounded 12.17% and 20.64% after binding site mutation ($p<0.0001$) (Figure 4f). IHC showed that 83.33% of p27 positive expression (5/6; Figure 4g-) showed in 6 low-level miR-590-3p expression clinical PC specimens, while 84.62% p27 negative expression(11/13; Figure 4g-) showed in 13 high-level miR-590-3p expression clinical PC specimens. 66.67% PPP2R2A positive expression (4/6; Figure 4g-) showed in 6 low-level miR-590-3p expression clinical PC specimens. The P value of OS between PC patients with positive PPP2R2A expression and negative PPP2R2A expression is bordering statistical significance (P=0.087, Figure 4h) and the former one had a better overall survival. Expression level of PPP2R2A was negatively connected with tumor size (P=0.017, Table 2).Statistical analysis indicated that miR-590-3p expression inverse relevant with p27 (P=0.004, Table 3) and PPP2R2A expression (P=0.025, Table 3).

Overexpression of P27 and PPP2R2A reversed the effect of miR-590-3p

To further confirm the role of p27 and PPP2R2A in mediating miR-590-3p, we performed rescue experiments. The p27 and PPP2R2A overexpression plasmids or plasmids of their corresponding empty vectors were transfected into PANC-1 cells, and the overexpression of p27 and PPP2R2A was confirmed by western blotting (Figure 5a). In order to determine the effect of overexpression of p27 and PPP2R2A on the action of miR-590-3p, we co-transfected the overexpression plasmid of p27 and PPP2R2A with miR-590-3p mimics into PANC-1 cells and observed the changes in cell function of PANC-1 cells co-transfected with no-load plasmid and miR-590-3p mimics. MTT and colony formation showed that overexpression of p27 and PPP2R2A significantly reduced the promoting effect of miR-590-3p on cell proliferation (Figure 5b and c). The overexpression of p27 and PPP2R2A also significantly reduced the promoting effect of miR-590-3p on cell migration and invasion (Figure 5d and e).

Disscussion

Hsa-miR-590-3p, one of the human microRNA-590 family, has been reported to be a crucial factor in several malignant tumors. However, the function of miR-590-3p in different tumors remains controversial. MiR-590-3p relatively high expressed in gastric carcinoma (GC) samples and was associated with tumor relapse in GC patients by direct regulating PPM1F[16]. MiR-590-3p motivated colon cancer cell growth and metastasis via Wnt/β-catenin signaling pathway and Hippo pathway[6; 17] and enhanced ovarian cancer proliferation and metastasis via targeting Cyclin G2, FOXA2 and FOXO3[18; 19]. However, miR-590-3p suppressed glioblastoma cell invasion, migration and EMT by targeting ZEB1 and ZEB2 [8].To our knowledge, there is no systematic report about its function in PC.

According to our study, PC tissues expressed significantly more miR-590-3p than paired normal pancreas (P=0.038). Moreover, the miR-590-3p expression level showed significant relationship with tumor size (P=0.042) and preoperative CA19-9 level (P=0.046), which indicated close relationship of miR-590-3p with aggressive tumor progression. *In vitro*, miR-590-3p overexpression can promote PC cell proliferation, invasion and migration (Figure 3). WB further showed that the negative relationship among miR-590-3p, p27 and PPP2R2A protein expression, and this relationship can also be observed in PC samples. The relative luciferase activity significantly decreased with overexpression of miR-590-3p, and this activity rebounded partially but not completely after binding site mutation (Figure 4f).These finding revealed that miR-590-3p can directly downregulated p27 and PPP2R2A via the predicted binding sites. However, hsa-miR-590-3p had a regulatory effect on luciferase expression in mutant type 3 'UTR transcript of p27 and PPP2R2A ($p<0.0001$). Other atypical binding sites existence and the indirect effect of hsa-miR-590-3p overexpression leading to target gene overall downregulation are two possible reasons to explain above results [20; 21].

As early as in 1999, It had been found that loss of p27 expression was significantly associated with poor prognosis of PC [12].P27 is also an independent prognostic marker of stage I–II pancreatic cancer [11]. Upregulation or activation of p27 inhibited the activation of cyclin E/CDK2 complex and inhibited G1/S in cancer cells, and cyclin E2 can interact with p27 to contribute to tumorigenesis [22]. P27 had been reported to be regulated by miR221 and miR222 to influence the biological behaviors of PC cells [23; 24], which means that p27 can be a typical target gene of miRNAs in malignant tumor cells. We use the flow cytometry assay and western blot assay to confirm that miR-590-3p may promote the proliferation of PC cells by pushing forward G1/S via p27- cyclin E/CDK2 axis (Figure 2 and Figure 4). We reversed the promoting effect of miR-590-3p on the proliferation, migration and invasion ability of PANC-1 cells through overexpression of p27 and PPP2R2A, further confirming the mediating effect of p27 and PPP2R2A as target genes of miR-590-3p in pancreatic cancer cells (Figure5)

PPP2R2A and ZO-1 was downregulated by overexpression of miR-590-3p in this study (Figure 4a and 4c). PPP2R2A is a negative modulator in PC and can be the target gene of other miRNAs [25; 26]. Breast cancers harboring PPP2R2A deletions are associated with worse OS [27]. In patients with acute myeloid leukemia(AML), PPP2R2A has been shown to dephosphorylate AKT at Thr-308 rendering it inactive, which means low expression of PPP2R2A related to a poorer prognosis in AML[28; 29]. The negative

modulator role of PPP2R2A has also been elaborated in HCC [30], ovarian cancer[31], colorectal cancer[32] and pancreatic cancer[24; 25]. In current study, PPP2R2A positive expression was closely related to a better OS of PC patients (P=0.087, Figure 4h). More clinical specimens will be added in our follow-up study.

Conclusion

In conclusion, we first found that miR-590-3p promotes the proliferation, migration and invasion of pancreatic cancer cells and miR-590-3p directly downregulated p27 and PPP2R2A and via the G1/S cell cycle pathway to promote the development of pancreatic cancer which may act as an oncomiR and may serve as a diagnostic and therapeutic target in PC.

Abbreviations

Abbreviations	Full name
BCA	Bicinchoninic acid
CDK2	cyclin-dependent kinases 2
DAB	Diaminobenzidine
DMEM	dulbecco's modified eagle's medium
DMSO	Dimethyl Sulfoxide
ECL	electrochemiluminescence
EDTA	Ethylene Diaminetetraacetic Acid
FBS	fetal bovine serum
GAPDH	glyceraldehyde-3-phosphate dehydrogenase
IHC	Immunohistochemistry
LB	Luria-Bertani/lysogeny broth
miR/miRNA	microRNA
MTT	Thiazolyl Blue Tetrazolium Bromide
p21	p21 Waf1/Cip1
p27	p27 Kip1
PBS	Phosphate Buffer Solution
PC	pancreatic cancer
PDAC	pancreatic ductal adenocarcinoma
PMSF	Phenylmethanesulfonyl Fluoride
PPP2R2A	Serine/threonine-protein phosphatase 2A 55 kDa regulatory subunit B alpha isoform
PVDF	polyvinylidene fluoride
qRT-PCR/PCR	Quantitative real-time Polymerase Chain Reaction
RIPA	Radio Immunoprecipitation Assay
RPMI-1640	Roswell Park Memorial Institute 1640
SDS	Sodium Dodecyl Sulfate
UICC	Union for International Cancer Control
WB	Western blot
ZO-1	Tight junction protein 1

Declarations

ETHICS APPROVAL AND CONSENT TO PARTICIPATE

This study was approved by the institutional review board of the China Medical University and a consent form was signed by each participating patient.

CONSENT FOR PUBLICATION

Written informed consent for publication was obtained from all participants.

AVAILABILITY OF DATA AND MATERIALS

All data included in this study are available upon request by contact with the corresponding author.

COMPETING INTERESTS

Not applicable

FUNDING

This work was supported by National Natural Science Foundation of China (No. 81672835).

AUTHORS' CONTRIBUTIONS

Xiaoyang Shi designed the experiment, completed most of experiments, analyzed the data and wrote the original drft. Weiwei Sheng helped to designe the experiment and edit the manuscript. Chao Jia and Jingtong Tang help to completed some of experiments. Ming Dong is the supervisor of the whole project.

ACKNOWLEDGMENTS

We thank the institute of general surgery and central laboratory of the First Hospital of China Medical University for technical support.

CONFLICTS OF INTEREST

The authors declare no conflict of interest.

References

[1] Ferlay J, Soerjomataram I, Dikshit R, et al. Cancer incidence and mortality worldwide: sources, methods and major patterns in GLOBOCAN 2012[J]. Int J Cancer, 2015, 136(5): E359-86.

[2] Bartel D P. MicroRNAs: genomics, biogenesis, mechanism, and function[J]. Cell, 2004, 116(2): 281-97.

[3] Ekhteraei-Tousi S, Mohammad-Soltani B, Sadeghizadeh M, et al. Inhibitory effect of hsa-miR-590-5p on cardiosphere-derived stem cells differentiation through downregulation of TGFB signaling[J]. J Cell Biochem, 2015, 116(1): 179-91.

[4] Lee S, Yu K R, Ryu Y S, et al. miR-543 and miR-590-3p regulate human mesenchymal stem cell aging via direct targeting of AIMP3/p18[J]. Age (Dordr), 2014, 36(6): 9724.

[5] Li Y, Sarkar F H. MicroRNA Targeted Therapeutic Approach for Pancreatic Cancer[J]. Int J Biol Sci, 2016, 12(3): 326-37.

[6] Feng Z Y, Xu X H, Cen D Z, et al. miR-590-3p promotes colon cancer cell proliferation via Wnt/beta-catenin signaling pathway by inhibiting WIF1 and DKK1[J]. Eur Rev Med Pharmacol Sci, 2017, 21(21): 4844-4852.

[7] Zhou C, Li J, Li J, et al. Hsa-miR-137, hsa-miR-520e and hsa-miR-590-3p perform crucial roles in Lynch syndrome[J]. Oncol Lett, 2016, 12(3): 2011-2017.

[8] Pang H, Zheng Y, Zhao Y, et al. miR-590-3p suppresses cancer cell migration, invasion and epithelial-mesenchymal transition in glioblastoma multiforme by targeting ZEB1 and ZEB2[J]. Biochem Biophys Res Commun, 2015, 468(4): 739-45.

[9] Hong L, Zhao X, Shao X, et al. miR-590 regulates WT1 during proliferation of G401 cells[J]. Mol Med Rep, 2017, 16(1): 247-253.

[10] Soos T J, Kiyokawa H, Yan J S, et al. Formation of p27-CDK complexes during the human mitotic cell cycle[J]. Cell Growth Differ, 1996, 7(2): 135-46.

[11] Juuti A, Nordling S, Louhimo J, et al. Loss of p27 expression is associated with poor prognosis in stage I-II pancreatic cancer[J]. Oncology, 2003, 65(4): 371-7.

[12] Lu C D, Morita S, Ishibashi T, et al. Loss of p27Kip1 expression independently predicts poor prognosis for patients with resectable pancreatic adenocarcinoma[J]. Cancer, 1999, 85(6): 1250-60.

[13] Feakins R M, Ghaffar A H. p27 Kip1 expression is reduced in pancreatic carcinoma but has limited prognostic value[J]. Hum Pathol, 2003, 34(4): 385-90.

[14] Janssens V, Goris J. Protein phosphatase 2A: a highly regulated family of serine/threonine phosphatases implicated in cell growth and signalling[J]. Biochem J, 2001, 353(Pt 3): 417-39.

[15] Lechward K, Awotunde O S, Swiatek W, et al. Protein phosphatase 2A: variety of forms and diversity of functions[J]. Acta Biochim Pol, 2001, 48(4): 921-33.

[16] Zhang J, Jin M, Chen X, et al. Loss of PPM1F expression predicts tumour recurrence and is negatively regulated by miR-590-3p in gastric cancer[J], 2018, 51(4): e12444.

[17] Sun Z Q, Shi K, Zhou Q B, et al. MiR-590-3p promotes proliferation and metastasis of colorectal cancer via Hippo pathway[J]. Oncotarget, 2017, 8(35): 58061-58071.

[18] Salem M, O'brien J A. miR-590-3p Promotes Ovarian Cancer Growth and Metastasis via a Novel FOXA2-Versican Pathway[J], 2018, 78(15): 4175-4190.

[19] Salem M, Shan Y, Bernaudo S, et al. miR-590-3p Targets Cyclin G2 and FOXO3 to Promote Ovarian Cancer Cell Proliferation, Invasion, and Spheroid Formation[J]. Int J Mol Sci, 2019, 20(8).

[20] Lorenz W W, Mccann R O, Longiaru M, et al. Isolation and expression of a cDNA encoding Renilla reniformis luciferase[J]. Proc Natl Acad Sci U S A, 1991, 88(10): 4438-42.

[21] Farr A, Roman A. A pitfall of using a second plasmid to determine transfection efficiency[J]. Nucleic Acids Res, 1992, 20(4): 920.

[22] Wingate H, Zhang N, Mcgarhen M J, et al. The tumor-specific hyperactive forms of cyclin E are resistant to inhibition by p21 and p27[J]. J Biol Chem, 2005, 280(15): 15148-57.

[23] Sarkar S, Dubaybo H, Ali S, et al. Down-regulation of miR-221 inhibits proliferation of pancreatic cancer cells through up-regulation of PTEN, p27(kip1), p57(kip2), and PUMA[J]. Am J Cancer Res, 2013, 3(5): 465-77.

[24] Li Z, Tao Y, Wang X, et al. Tumor-Secreted Exosomal miR-222 Promotes Tumor Progression via Regulating P27 Expression and Re-Localization in Pancreatic Cancer[J]. Cell Physiol Biochem, 2018, 51(2): 610-629.

[25] Wang Q, Li J, Wu W, et al. Smad4-dependent suppressor pituitary homeobox 2 promotes PPP2R2A-mediated inhibition of Akt pathway in pancreatic cancer[J]. Oncotarget, 2016, 7(10): 11208-22.

[26] Shen R, Wang Q, Cheng S, et al. The biological features of PanIN initiated from oncogenic Kras mutation in genetically engineered mouse models[J]. Cancer Lett, 2013, 339(1): 135-43.

[27] Beca F, Pereira M, Cameselle-Teijeiro J F, et al. Altered PPP2R2A and Cyclin D1 expression defines a subgroup of aggressive luminal-like breast cancer[J]. BMC Cancer, 2015, 15: 285.

[28] Shouse G, De Necochea-Campion R, Mirshahidi S, et al. Novel B55alpha-PP2A mutations in AML promote AKT T308 phosphorylation and sensitivity to AKT inhibitor-induced growth arrest[J]. Oncotarget, 2016, 7(38): 61081-61092.

[29] Ruvolo P P, Ruvolo V R, Jacamo R, et al. The protein phosphatase 2A regulatory subunit B55alpha is a modulator of signaling and microRNA expression in acute myeloid leukemia cells[J]. Biochim Biophys Acta, 2014, 1843(9): 1969-77.

[30] Wong Q W, Ching A K, Chan A W, et al. MiR-222 overexpression confers cell migratory advantages in hepatocellular carcinoma through enhancing AKT signaling[J]. Clin Cancer Res, 2010, 16(3): 867-75.

[31] Zhang J, Gao D, Zhang H. Upregulation of miR-614 promotes proliferation and inhibits apoptosis in ovarian cancer by suppressing PPP2R2A expression[J]. Mol Med Rep, 2018, 17(5): 6285-6292.

[32] Liang W L, Cao J, Xu B, et al. miR-892a regulated PPP2R2A expression and promoted cell proliferation of human colorectal cancer cells[J]. Biomed Pharmacother, 2015, 72: 119-24.

Tables

Table 1. Clinicopathological Associations of miR-590-3p Expression in Primary PC

Clinicopathological	no. of patients	Expression of miR-590-3p		χ2	P
parameters		high	low		
Cases	42				
Age(years)					
≤60	27	16	11	0.224	0.636
60	15	10	5		
Gender					
Male	24	15	9	0.008	0.927
Female	18	11	7		
Tumor location					
Head	31	20	11	0.342	0.559
Body-tail	11	6	5		
Tumor size(cm)					
2.5	11	4	7	4.123	0.042*
≥2.5	31	22	9		
Differention					
Well	18	12	6	0.303	0.582
Moderate and poor	24	14	10		
UICC stage					
+a	30	20	10	1.01	0.315
B+	12	6	6		
Lymph nodes metastasis					
N0(negative)	30	20	10	1.01	0.315
N1+N2(positive)	12	6	6		
Pre-therapeutic CA19-9					
level(U/ml)					
37	9	3	6	3.965	0.046*
≥37	33	23	10		
Postoperative liver metastasis					

Negative	24	17	7	1.893	0.169
Positive	18	9	9		

miR-590-3p expression higher and lower than the mean expression level was defined as high and low expression, respectively; *P<0.05, statistically significant.

Table 2. Clinicopathological Associations of PPP2R2A Expression in Primary PC

Clinicopathological	no. of patients	PPP2R2A		χ2	P
parameters		positive	negative		
cases	60	12	48		
Age(years)					
≤60	35	8	27	0.429	0.513
60	25	4	21		
Gender					
Male	34	8	26	0.611	0.434
Female	26	4	22		
Tumor location					
Head	43	7	36	1.313	0.252
Body-tail	17	5	12		
Tumor size					
2.5	18	7	11	5.734	0.017*
≥2.5	42	5	37		
Differentiation					
Well	19	3	16	0.308	0.579
Moderate and poor	41	9	32		
T stage					
T1+T2	55	11	44	0	1
T3+T4	5	1	4		
Lymph nodes metastasis					
N0(negative)	48	10	38	0.104	0.747
N1positive	12	2	10		
UICC stage					
+a	45	10	35	0.556	0.456
B+	15	2	13		

Pre-therapeutic CA19-9 level(U/ml)					
<37	12	4	8	1.667	0.197
≥37	48	8	40		
Postoperative liver metastasis					
Negative	35	8	27	0.429	0.513
Positive	25	4	21		

Table 3. Expression Association Between miR-590-3p and p27 and PPP2R2A (n=19) in PC

	Expression of miR-590-3p		
	High expression (n=13)	Low expression (n=6)	P value
p27			
Positiv	2	5	0.004
Negative	11	1	
PPP2R2A			
Positiv	2	4	0.025
Negative	11	2	

Figures

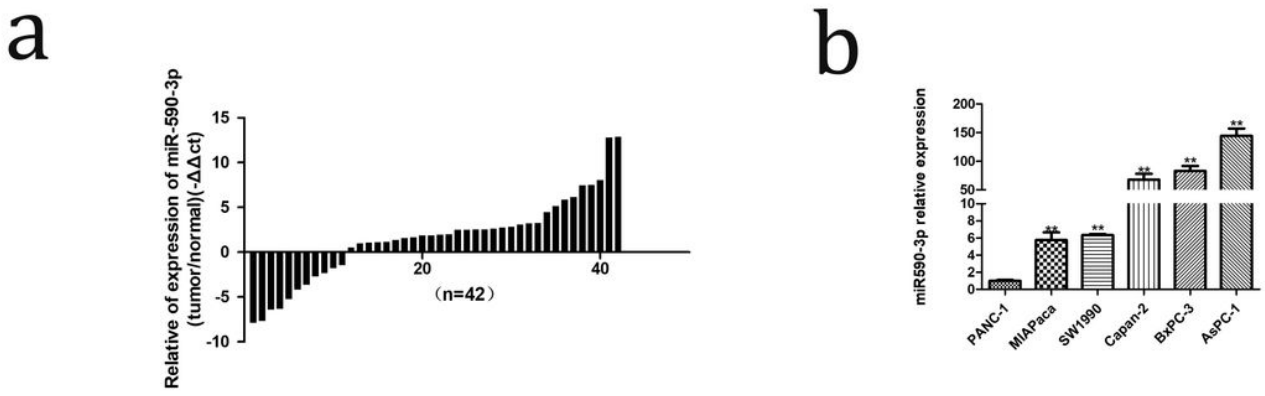

Figure 1

MiR-590-3p expression in tissue samples and in PC cells. (a) miR-590-3p expression quantities in tissue samples were quantified by qPCR (normalized to U6 snRNA). 2-ΔΔct values represent relative expression

level. (b) Expression quantities of miR-590-3p in different PC cells. Bars indicate±S.E.**P<0.01.

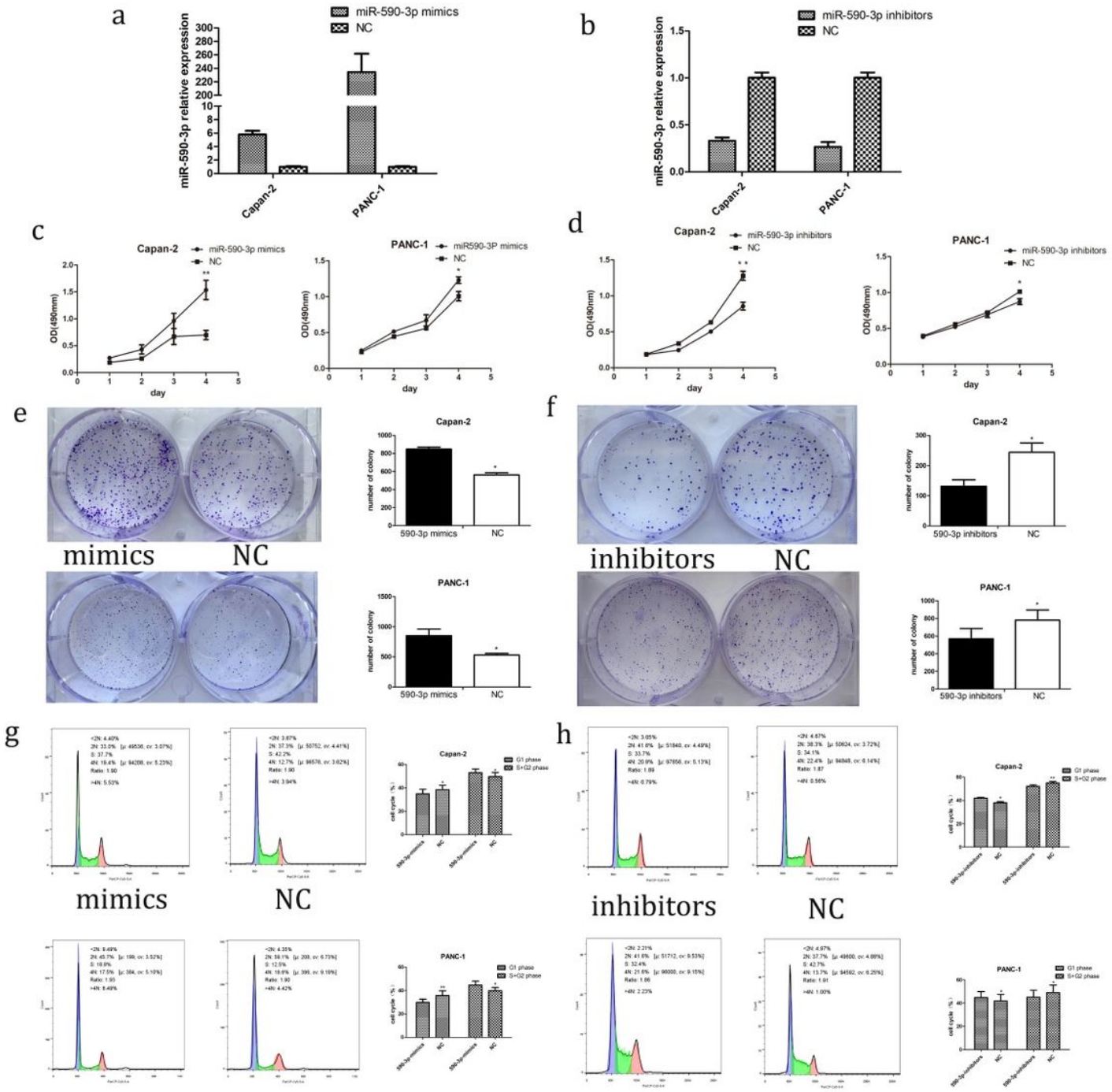

Figure 2

MiR-590-3p enhanced cancer cell proliferation in vitro via altering cell cycle profiles. (a) and (b) Transfection efficiency of miR-590-3p mimics and inhibitors in two PC cells quantified by qPCR. (c) and (d) Cell proliferation in the two PC cells under the condition of miR-590-3p overexpression and downregulation. (e) and (f) Colony formation in the two PC cells under the condition of miR-590-3p

overexpression and downregulation (g) and (h) Cell cycle profiles of two PC cells under the condition of miR-590-3p overexpression and downregulation. *P<0.05, ** P<0.01.

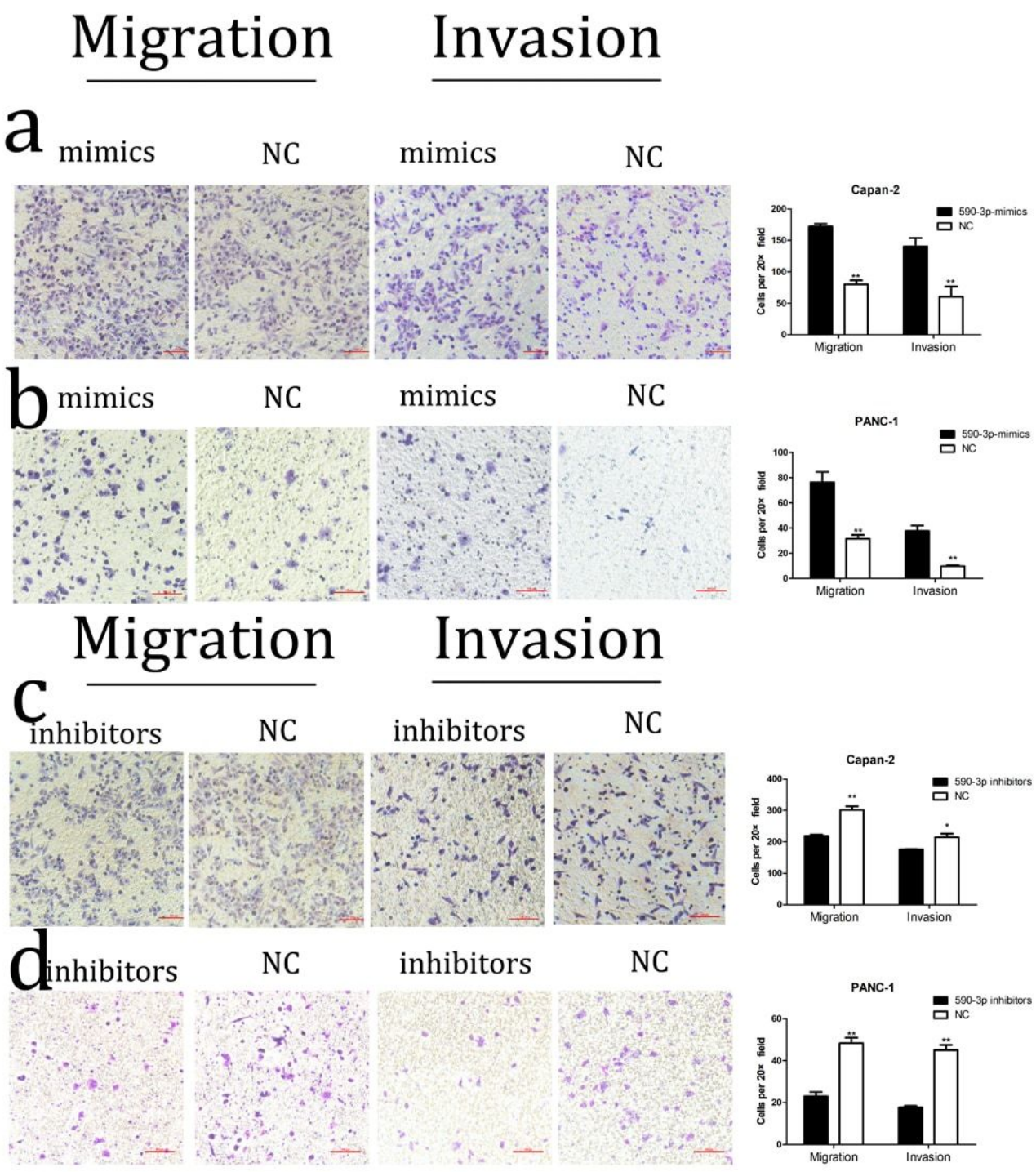

Figure 3

MiR-590-3p promoted PC cell migration and invasion. (a) Capan-2 cell migration and invasion under the condition of miR-590-3p overexpression and downregulation. *P<0.05, ** P<0.01. (b) PANC-1 cell migration and invasion after transfected with the miR-590-3p mimics or NC *P<0.05, ** P<0.01. (c)

Capan-2 cell migration and invasion under the condition of miR-590-3p overexpression and downregulation. *P<0.05, ** P<0.01. (d) PANC-1 cell migration and invasion under the condition of miR-590-3p overexpression and downregulation. *P<0.05, ** P<0.01.

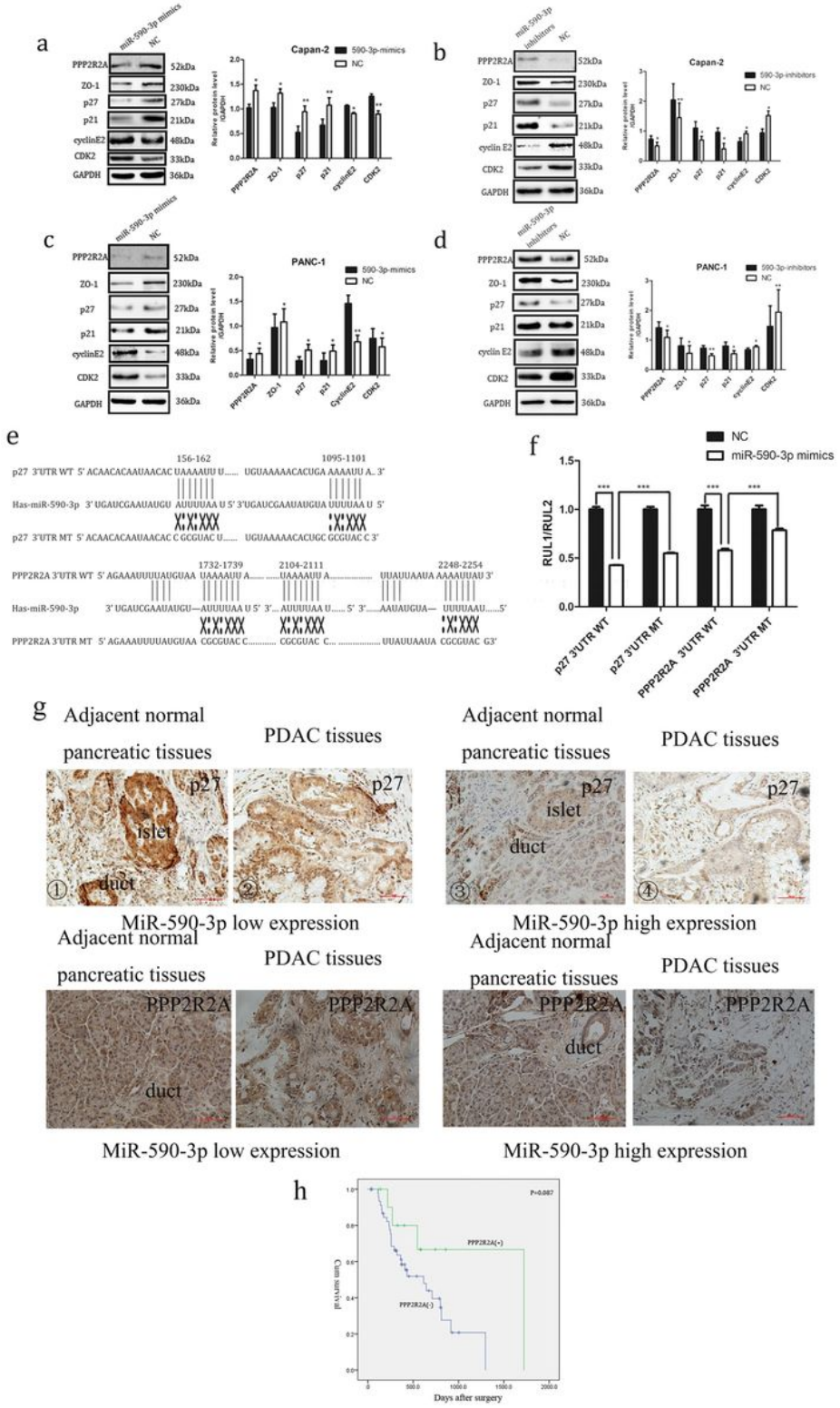

Figure 4

MiR-590-3p directly targets the 3'-UTR of p27 and PPP2R2A. (a)- (d) P27, PPP2R2A and other related protein expression was examined by a western blot assay in two PC cells. *P<0.05, ** P<0.01. (e) MiR-

590-3p and its possible binding sites on the 3’-UTR of p27 and PPP2R2A. WT, wild type. MT, mutant type. (f) Relative luciferase intensity in HEK-293 cells cotransfected with miR-590-3p or NC and p27 and PPP2R2A luciferase reporter plasmid. Data are showed as the ratio of firefly intensity to Renilla luciferase intensity. (g) -different expression intensities of p27 within low or high expression of miR-590-3p. -different expression intensities of PPP2R2A with low or high miR-590-3p expression.*P<0.05, ** P<0.01, *** P<0.001.

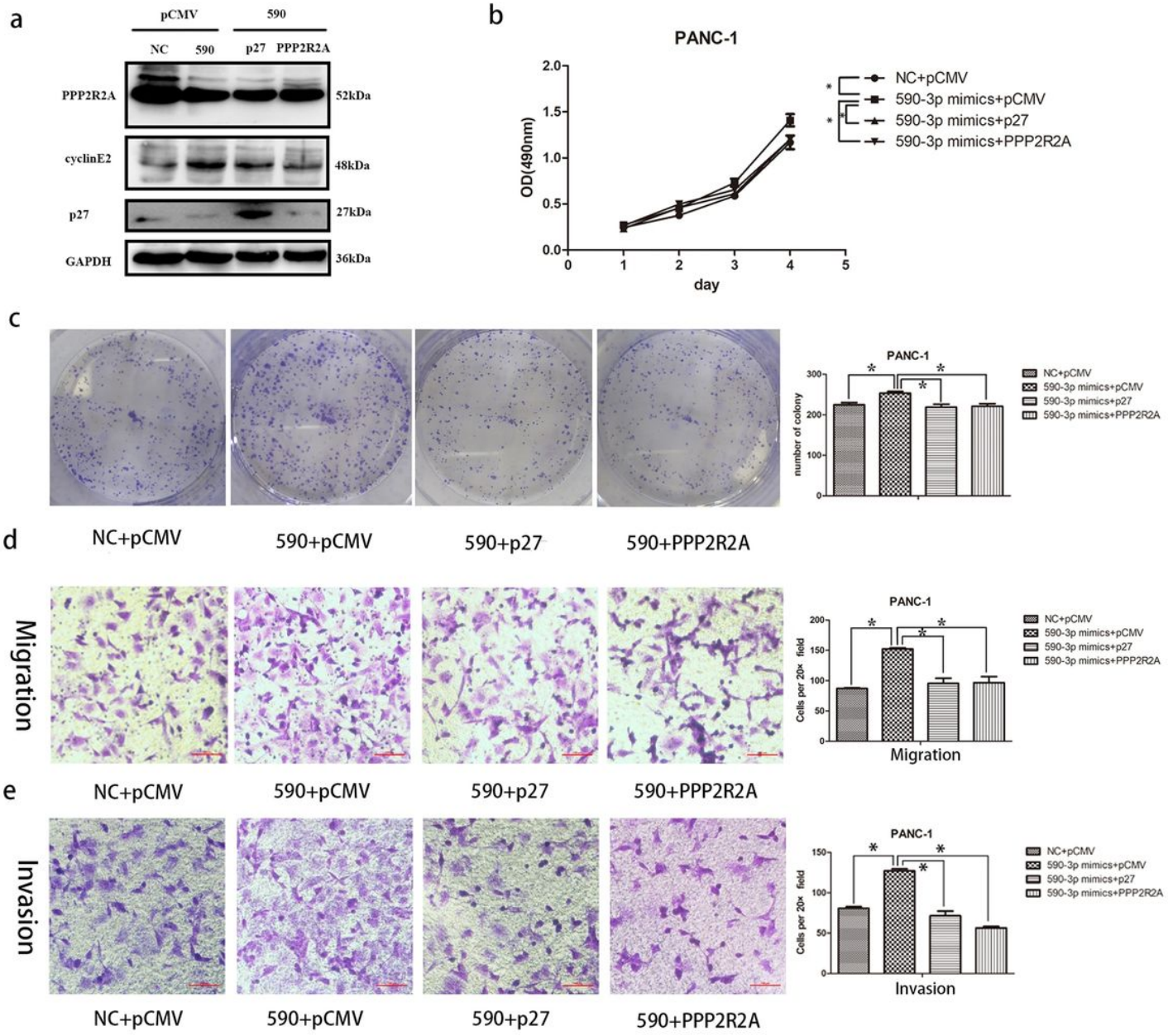

Figure 5

The overexpression of p27 and PPP2R2A reversed the promoting effect of miR-590-3p on the proliferation, migration and invasion ability of PANC-1. (a) WB confirmed the overexpression of p27 and PPP2R2A. (b)The proliferation capacity of PANC-1 cells co-transfected with p27, PPP2R2A and miR-590-3p mimics was significantly lower than that of PANC-1 cells co-transfected with pCMV and miR-590-3p mimics.(c)PANC-1 cells co-transfected with p27, PPP2R2A and miR-590-3p mimics and co-transfected with pCMV and miR-590-3p mimics were determined for colony formation. (d)PANC-1 cell migration experiment in which pCMV and miR-590-3p mimics were co-transfected with PANC-1 cells co-transfected with p27, PPP2R2A and mir-590-3p mimics.(e)PANC-1 cell invasion experiment in which pCMV and miR-590-3p mimics were co-transfected with PPP2R2A and miR-590-3p mimics, * $P < 0.05$.